REMOTE SENS. ENVIRON. 27:1–10 (1989)

Measurements of Short-Term Thermal Responses of Coniferous Forest Canopies Using Thermal Scanner Data

J. C. Luvall
H. R. Holbo
Science and Technology Laboratory,
NASA Stennis Space Center

Thermal Infrared Multispectral Scanner (TIMS) data were collected over the H. J. Andrews Experimental Forest, a coniferous forest in western Oregon. TIMS flights were timed to coincide with solar noon. Flight lines were overlapped with a 28-min time difference between flight lines. Concurrent radiosonde measurements of atmospheric profiles of air temperature and moisture provided inputs to LOWTRAN6 for atmospheric radiance corrections of the TIMS data. Surface temperature differences measured by the TIMS over time between flight lines were combined with surface radiative energy balance estimates to develop thermal response numbers (TRN). These numbers characterized the thermal response ($kJm^{-2}°C^{-1}$) of the different surface types. Barren surfaces had the lowest TRN whereas the forested surfaces had the highest.

Address correspondence to Dr. J. C. Luvall, Science and Technology Lab., HA10, Stennis Space Center, MS 39529.
Received 4 February 1988; revised 28 October 1988.

0034-4257/89/$0.00

INTRODUCTION

Investigations using thermal infrared measurements to study the biophysical response of vegetated surfaces to environmental factors have been conducted since the 1960s (Gates, 1962). Most research since then has focused on agricultural crops and soils. Estimates of soil moisture, plant moisture stress, crop yields, and evapotranspiration have been made using a wide variety of satellite-, aircraft-, and ground-based thermal sensors (Soer, 1980; Price, 1980, 1982; Idso et al., 1975; Seguin and Itier, 1983; Stone and Horton, 1974; Hatfield et al., 1984, Heilman et al., 1976; Reginato et al., 1985; Jackson et al., 1977; Idso et al., 1977).

Applications of aircraft-based thermal sensors in forestry have primarily involved spotting forest fires and the use of uncalibrated imagery for detecting cold air drainage patterns in mountain terrain (Hirsh et al., 1971; Fritschen et al., 1982; Balick and Wilson, 1980). Recent work by Sader (1986) used the calibrated aircraft-mounted sensor TIMS (Thermal Infrared Multispectral Scanner) to measure the effective radiant temperatures of coniferous forests in western Oregon.

On a global scale, climate modelers are beginning to include the important linkages between different kinds of land surface and the atmosphere as factors influencing global patterns of rainfall, of temperature, and of atmospheric circulation (Shukla and Mintz, 1982). These linkages have yet to be fully characterized in global models of atmospheric processes. Global Climate Models (GCM) suffer from a lack of detail about how different surfaces respond thermally, and, hence, affect local climatic processes. These models could be improved by using thermal infrared measurements to quantify the biophysical response of the surface in relation to environmental energy fluxes (radiative, latent, conductive, and convective). Information at larger spatial resolution is also needed by the global modelers for improving their predictive capabilities (Carson, 1982), since the heterogeneity in surface types makes it difficult to characterize averages over the smaller spatial resolution used in global climate models (Dickinson, 1983).

The thermal response of a land surface is dependent on complex interactions between many physical and vegetation factors. In agricultural areas and grasslands, the amount of vegetation cover, its composition, and soil moisture all influence the thermal response (Carlson, 1986). Forested landscapes result in a very complex situation. The thermal response of a forested landscape may involve as little as a few centimeters of soil, such as in clearcuts, to as much as tens of meters of air and biomass above the soil, such as in old growth forests. These differences in forest structure present a complex range of surfaces for which the thermal response may depend primarily upon soil properties, at one extreme, and upon forest canopy type, depth, and architecture, at the other. Also, many forests occur in rugged mountain terrain, so that ground slope and aspect become important determinants, particularly in controlling radiant energy fluxes.

In remote sensing, temporal changes in the amount of emitted thermal radiation, i.e., temperature differences, have often been employed to estimate surface properties (Pohn et al., 1974; Kahle, 1987; Schieldge et al., 1980; Ho, 1987). The surface property addressed by these workers is called the thermal inertia (Price, 1977):

(1) Thermal inertia ($cal/cm^2\,°C\,s^{0.5}$):

$$P = (1/\rho c\lambda)^{0.5},$$

where ρ is density (g/cm^3), c is specific heat ($cal/g\,°C$), and λ thermal conductivity ($cal/cm\,s\,°C$). As can be seen, P includes three fundamental properties of soils (Sellers, 1965; Monteith, 1973).

The time difference between surface temperature observations used in these earlier studies was usually preestablished by the orbital mechanics of the satellite, typically 12 h. Thus, all of the P estimation algorithms are needed to make allowances for surface dynamics during the intervening portion of the diurnal (cyclic) period. This involved either flux estimates using surface measurements, or modeling of the surface energy fluxes, including the fluxes of sensible and latent heat, the net radiation balance, and the subsurface heat conduction. Fourier techniques were commonly invoked in describing the cyclic nature of these variables.

In terms of the types of surface they could accommodate, these approaches are limited to surfaces for which the models could be formulated, where suitable values for the specific heat capacity and thermal conductivity can be chosen or derived, and which were homogeneous in these properties at the spatial scale of the estimate. As a result, P estimates for partially vegetated or canopied surfaces were not generally attempted.

It is recognized that total heat storage can be an important term (up to 10% of daily net radiation and $\geq 50\%$ near sunrise and sunset) in the energy budget of forest canopies and canopy heat storage can equal soil heat storage when soil moisture is $< 20\%$ (Moore, 1976; Moore and Fisch, 1986; McCaughey, 1985). However, it is difficult to determine heat storage rates in forested terrain (Moore and Fisch, 1986; McCaughey, 1985; Stewart and Thom, 1973; Thom, 1975). The direct method used for estimating canopy heat storage is to integrate temperature change rates from a large number of air and biomass temperature measurements throughout the canopy space (Aston, 1985). An alternative method relies on fewer canopy temperature measurements in combination with soil heat flux estimates, estimated specific heats of the biomass, and net radiation measurements (McCaughey, 1985; Moore and Fisch, 1986). These techniques for determining canopy heat storage and temperature response are limited to site-specific studies employing intensive ground-based measurements, and cannot be extrapolated to other

forests with differing canopy structure and biomass (Moore and Fisch, 1986).

However, Sader (1986) used TIMS to demonstrate that thermal radiation measures were linked to the physical structure of forest stands. He found that different Douglas-fir forest stands at the Andrews Experimental Forest yielded different surface temperatures, depending on their composition and amount of green biomass. His work indicated that forest stands greater than 25 years of age had lower canopy temperatures than younger, less dense stands. Also, aspect and slope were found more important in determining canopy temperatures for younger stands than for older stands.

OBJECTIVE

A technique is needed to examine forest canopy thermal response which avoids the dynamic complexity of the modeling approaches and/or the intensive temperature measurements taken throughout the forest canopy, yet accounts for the effects of the canopy structure and the environmental energy fluxes. The approach should not require site-specific measurements and be able to examine many surface types throughout a forested landscape. The objective of this study was to use the change in surface temperature as measured by the TIMS over short time periods, coupled with solar and long-wave radiation measurements, to express the effects of surface heat storage rates, from various surface types to characterize the thermal response of forested landscapes.

METHODS

A Thermal Response Number

We will assume that a change in surface temperature can be regarded as an aggregate expression of both surface properties (canopy structure and biomass, age, and physiological condition) and environmental energy fluxes (solar and long wave radiation; sensible and latent heat). Over short time intervals, it is not unreasonable to assume that environmental energy fluxes proceed at constant, unchanging rates, at least during periods of fair weather. This relieves the need to model flux dynamics during the TIMS measurement interval. Making this assumption, we can use surface net radiation as the value which essentially integrates the effects of the nonradiative fluxes, and the rate of change in surface temperature as the value which reveals how those nonradiative fluxes are reacting to radiant energy inputs. Their ratio can be used to define a surface property we call a Thermal Response Number (TRN):

(2) Thermal response number ($Jm^{-2}°C^{-1}$):

$$\mathrm{TRN} = \frac{\sum_{t_1}^{t_2}(R_n * \Delta t)}{\Delta T}.$$

(3) Mean polygon temperature for each surface type:

$$T = \frac{\Sigma(T_p)}{n},$$

where $\sum_{t_1}^{t_2}(R_n * \Delta t)$ ($\mathrm{J\,m^{-2}}$) is the total net radiation of the site between flights t_1 and t_2, Δt time between flights, and T the mean surface temperatures (spatially averaged), T_p the pixel temperature, n the number of pixels in the surface type, and ΔT its change in surface temperature for the same period of time.

Radiation Balance

One minute averages of incoming solar (Li-Cor[1] pyranometer 0.4–1.1 μm) and longwave radiation (Eppley pyrgeometer[2] 5–50 μm) were measured during the flight period. The net all-wave radiation balance ($\mathrm{W\,m^{-2}}$) of each surface was estimated for the TRN time period using:

(4) Net solar:

$$K^* = (1 - \alpha)\phi(K\downarrow).$$

(5) Net longwave:

$$L^* = L\downarrow - \varepsilon\left[\sigma(T)^4\right].$$

(6) Net allwave radiation:

$$R_n = K^* + L^*.$$

[1]Li–Cor, Lincoln, NE.

[2]Eppley Lab, Newport, RI. Use of trade names implies no endorsement by NASA.

Here $K\downarrow$ is the measured incoming solar radiation, ϕ a site-dependent slope and aspect solar gain coefficient (Garnier and Ohmura, 1968), α site albedo, $L\downarrow$ measured incoming longwave radiation, $L\uparrow$ calculated outgoing longwave radiation using ε the surface emissivity (0.99), σ the Stefan–Boltzman constant ($5.7 * 10^{-8}\,W m^{-2} T^{-4}$), and T average surface temperature in degrees Kelvin. Site albedo for the clearcut was determined for clearcuts similar to those at the Andrews (Holbo and Childs, 1987). Other albedos were obtained from literature values (Jarvis et al., 1976; McCaughey, 1987; Dickinson, 1983). The range of emissivity of vegetation canopies ranges from 0.94 to 0.99 (Monteith, 1973) and soils from 0.95 to 0.99 (Taylor, 1979). Generally values of emissivity in the 8–14 μm range for vegetated surfaces do not deviate significantly from unity (Oke, 1978; Dickinson, 1983; Carlson, 1986).

(7) The thermal energy budget ($W m^{-2}$) can be expressed:

$$R_n = H + LE + G.$$

In this equation, R_n, net radiation, is the amount of energy transformed at the surface into nonradiative processes at the surface, H sensible heat flux, LE latent heat flux, and G energy flux into the soil. From Eq. (7) it can be seen that R_n expresses the combined energies of the nonradiative surface processes, making it the appropriate reference value for ΔT in the TRN.

TIMS Data Collection and Analysis

The Thermal Infrared Multispectral Scanner (TIMS) is an aircraft mounted instrument (Palluconi and Meeks, 1985). It was employed to obtain the measurements needed for investigating forest canopy thermal response, and in the development of an analytical modeling technique of that thermal response. The TIMS has six thermal channels in the wavelength regions of 8.2–12.2 μm. The TIMS usable swath width is $\pm 30°$ of nadir. Since radiance measures from all six channels were highly correlated, only Channel 2 (8.4–9.2 μm) was used in this study. The TIMS is a calibrated thermal scanner with a noise equivalent temperature (NE ΔT) of 0.09°C for Channel 2. A precision of 0.2°C is obtained over the temperature range of 10–65°C. Preflight optical bench calibrations were obtained for the TIMS spectral response and blackbody temperature settings. Calibrated temperature readings are possible because of on-board low and high temperature blackbodies. The blackbody temperatures are selected to bracket the expected range of surface temperatures to optimize TIMS temperature resolution.

On 5 August 1985, TIMS overflights were flown at 13:37 local time (solar noon 13:12) with an average nadir ground resolution of 10 m pixel size. Flights were planned to cover the area during the time of maximum solar irradiance. Flight paths were overlapped with 28.3 min time difference between flight lines to examine the short term changes in surface temperatures. All areas from which forest types were chosen were within 10° of TIMS nadir.

An atmospheric profile from 436 to 10912 m of temperature, pressure (altitude), and relative humidity was measured by radiosonde after the TIMS flights. The atmospheric profile was incorporated in the LOWTRAN6 model for calculation of atmospheric radiance (Kneizys et al., 1983). Atmospheric longwave radiance values calculated by an earlier version, LOWTRAN5, have been shown to be in excellent agreement with measured atmospheric radiance values (Sweat and Carroll, 1983). Wilson and Anderson (1986) indicated the validity of using LOWTRAN5 for atmospheric radiance corrections of aircraft thermal data collected over short atmospheric path lengths.

The output from LOWTRAN6 was combined with calibrated TIMS spectral response curves and blackbody information recorded during the flight to produce a lookup table for pixel temperatures as a function of TIMS values (Anderson, 1985).

Flight lines were georeferenced to assure comparibility of each of the five areas between the flights. Areas representing the five surface types were extracted for further processing.

STUDY AREA

The H. J. Andrews Experimental Forest is 6500 ha. watershed located in the central-western Cascade Mountains of Oregon east of Eugene, OR. It is one of the National Science Foundation's longterm ecological research sites. It represents the dense coniferous forests of Douglas fir, western hemlock, and common true firs of the western slopes of the Cascade Mountains (Hawk et al.,

1978). Geological parent materials range from older andesites to younger basalts. Prior to selection as an ecological site, it had been used as a U.S. Forest Service Experimental Forest since 1948. It provides a wide range of forest stand ages, as well as logging, thinning, regeneration, and other kinds of forest land management practices.

Five forest stands were selected for this study, representing a range of forest canopy types and treatments for which different thermal responses could be expected. They are:

- A mature forest stand (MATUREF) with a canopy dominated by dense crowns of *Pseudotsuga menziesii* (Mirb.) Franco, a secondary canopy of dense *Tsuga heterophylla* (Raf.) Sarg., and a tall shrub layer of *Acer circinatum* Pursh. (Hawk et al., 1978). The average aspect of this site is southeast, 17% slope, at an elevation of 1080 m.
- A recent clearcut area (CLRCUT) that was harvested in the summer 1981 and was originally classified in the *Tsuga heterophylla-Abies amabilis* (Dougl.) species zone. Site aspect is south-southwest with a 20% slope, and an elevation of 853 m. It was burned to clear logging debris in August 1982, and planted in March 1983 with 1-year-old Douglas-fir seedling stock on a 3×3 m spacing. Fireweed (*Epilobium augustifolium* L.) is the predominant vegetative cover. The Douglas-fir seedlings are not yet a significant part of the site's cover. Logging debris constitutes about 10% of the emitting surface.
- A naturally regenerating forest (NATREG) that was clearcut-logged in 1955 and was originally in the *Tsuga heterophylla-Abies amabilis* species zone. The aspect is south with an 40% slope at a elevation of 869–1082 m. The site is the lower end of a small watershed, and supports a canopy of about 40% *A. circinatum* and 60% *P. menziesii*. There are openings in the canopy, exposing dry organic materials, and occasional rock outcroppings.

Figure 1. Atmospheric profiles of air and dew point temperatures from radiosonde data and used in LOWTRAN6 models for atmospheric radiance.

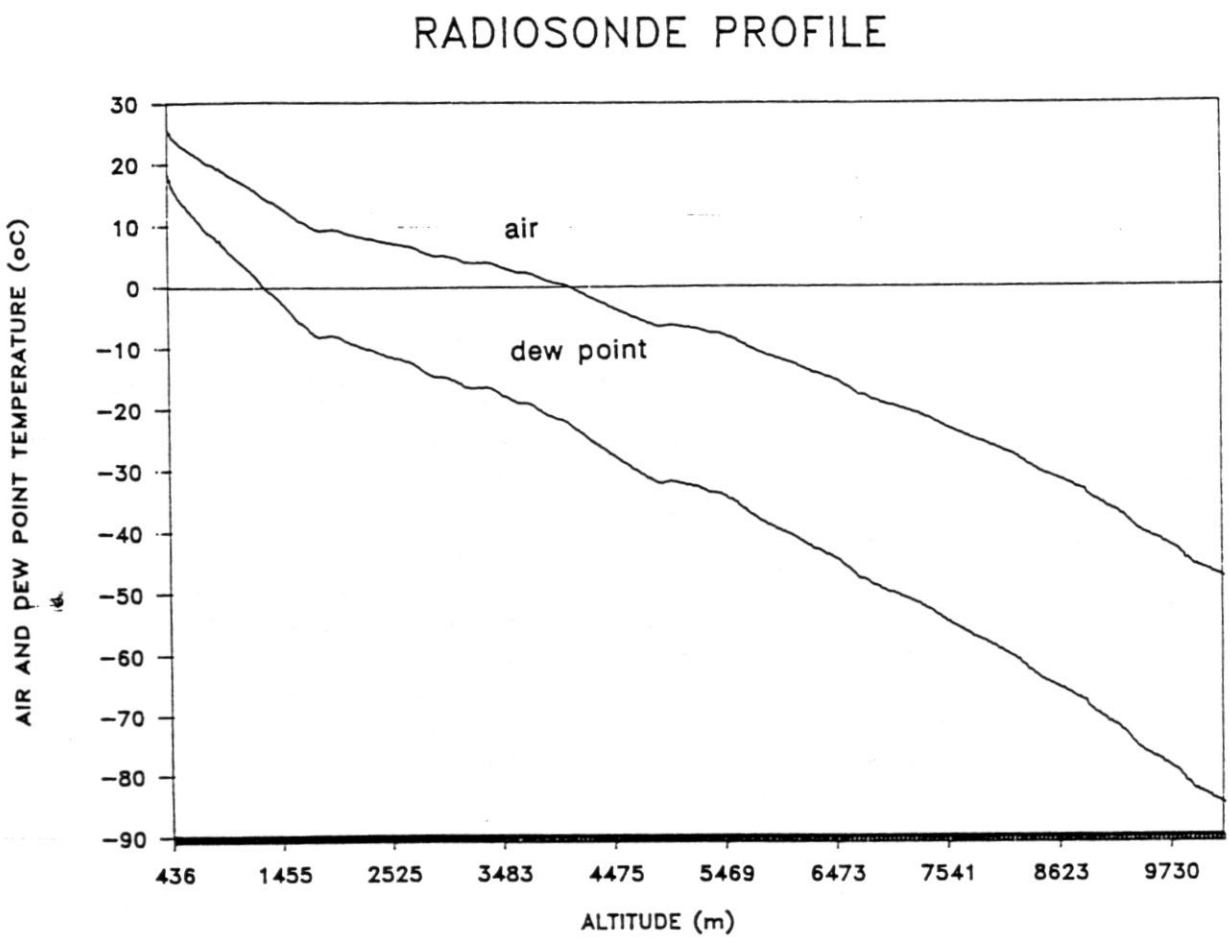

A Douglas-fir plantation (PLANT) that was clearcut-logged in the summer of 1953, and was originally classified within the *Tsuga heterophylla-Abies amabilis* species zone. It was planted in the fall of 1953 at a stocking rate of about 700 trees per acre, and interplanted to fill gaps in November 1963. The aspect is southeast with a 20% slope at a elevation of 838–914 m. Canopy coverage is fairly complete, although crown closure has not occurred, and thickets of Snowbrush (*Ceanothus cordulatus* Kell.) are common.

A quarry (QUARRY) is an area of barren rock used for road gravels. This exposed outcrop is composed of altered andesites at an elevation of 807 m.

RESULTS AND DISCUSSION

The data collection period was a clear and cloudless day (Figs. 1 and 2). $K\downarrow$ was approximately 75% of the solar constant at the time of TIMS overflights. $L\downarrow$ from the atmosphere was about 37% of the amount contributed by solar radiation. The atmospheric profiles of air and dew point temperature showed boundary layer gradients of $-0.007°C\ m^{-1}$ and $-0.003°C\ m^{-1}$, respectively. Profile slopes also showed no evidence of clouds or inversions. These conditions maximized daytime solar loading and provided uniform, nearly constant $K\downarrow$ flux to all study sites. Thus the T and ΔT of the various surface types depended entirely on how their R_n was partitioned among LE, H, and G.

Surfaces exhibited considerable differences in their radiation balances, average temperature, and changes in average temperatures (Table 1). The forested surfaces had greater R_n values than the clearcut or quarry. The mean surface temperature T and surface temperature change ΔT were different for each type of surface. One can note the inverse relationship between the amount of energy required to change surface temperature and factors like forest type, forest canopy volume, and the completeness of canopy cover. Both T and ΔT tended to increase with decreasing forest cover. It was evident that the presence of a forest canopy cover could significantly alter the thermal responses of the surfaces in two ways.

First, the forest canopy provides a mechanism for moderating solar irradiance to the soil surface beneath the canopy (Childs et al., 1985; Holbo et al., 1985). Vanderwaal and Holbo (1984) showed that Douglas-fir needle temperatures tracked air temperatures very closely (within 3°C), regardless of radiant fluxes and stomatal conductances. However, sunlit soil surface temperatures directly under the seedlings were 30–50°C higher than needle temperatures. Without a forest canopy as cover, the CLRCUT site surface temperatures would be greater than a forested surface for a given energy input.

Second, $L\uparrow$ (T) was greater for the CLRCUT and QUARRY sites than for the forested sites (NATREG, PLANT, and MATUREF), reducing the amount of R_n which would be available for partitioning among LE and G. Since the QUARRY site had no vegetative cover and the CLRCUT was mostly bare soil, LE was not a significant energy flux. It was apparent that only a small amount of energy was partitioned into G for these sites because of the magnitude of ΔT between flights. The forested sites had a greater R_n, yet T and ΔT were much smaller. It was evident that the sites with a forest canopy efficiently dissipated the energy. With large canopy biomass and surface area, forest R_n would be dissipated through either LE or H. However in coniferous forests, LE can proceed without producing much drop in T, and it is possible that H is the dominant mechanism for dissipating R_n (Jarvis et al., 1976). It is also possible that G could be significant, given the large canopy biomass of the forested sites. In coniferous forests, up to 10% of R_n can be allocated to G (Moore, 1976; McCaughey, 1985).

This study represents the first time that short term (e.g., 28 min) surface thermal response changes have been measured on a "landscape scale" for forests using remote thermal sensors. Each surface type produced a characteristically different TRN (Table 1). The sites could be ranked by using the TRN value. The TRN for the forested sites was much greater than for the QUARRY and CLRCUT sites. The TRN even differentiated among the forested sites. It was evident that one could not distinguish between the PLANT and NATREG sites by using only T. It is possible for two different forest canopies to have the same T, but partition the energy differently. Only when

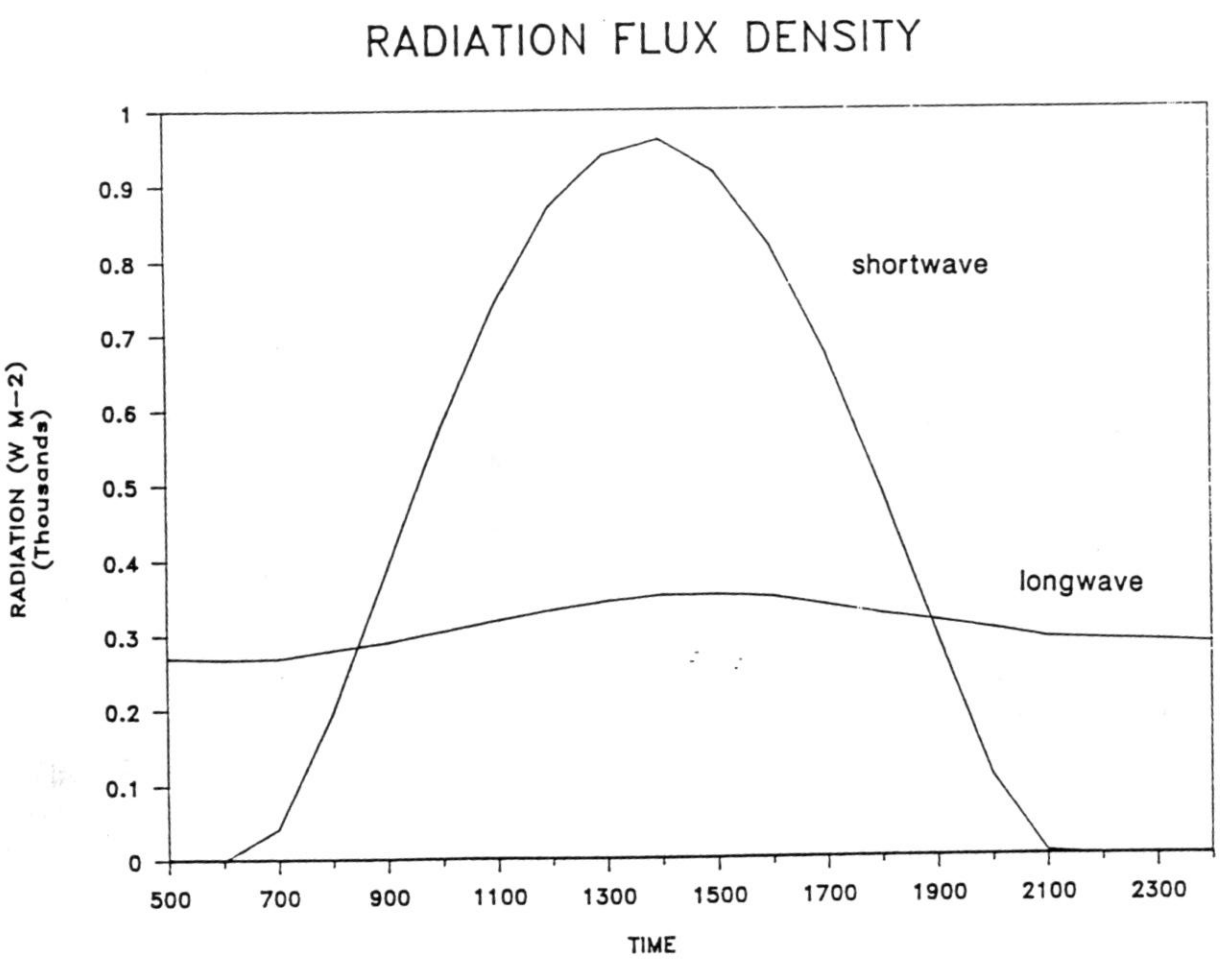

Figure 2. Shortwave and longwave radiation flux density during study period.

Table 1. Radiation Balance Estimates and Thermal Response Numbers for Various Forest Surface Types[a]

	Quarry	*Clrcut*	*Plant*	*Natreg*	*Matureg*
Albedo α	0.25	0.22	0.15	0.15	0.08
Solar gain ϕ	1.00	1.07	1.05	1.10	1.05
$K\downarrow$ (W m^{-2})	957	1024	1005	1053	1005
K^* (W m^{-2})	718	799	854	895	924
$L\downarrow$ (W m^{-2})	353	353	353	353	353
$L\uparrow$ (W m^{-2})	626	634	477	477	448
L^* (W m^{-2})	− 273	− 281	− 124	− 124	− 95
R_n (W m^{-2})	445	517	730	771	830
T (°C)	50.7	51.8	29.5	29.4	24.7
ΔT (°C)	4.50	2.16	0.76	1.66	0.91
$\Delta T/\Delta t$ (°C min^{-1})	0.16	0.08	0.03	0.06	0.03
TRN (kJ m^{-2} °C)$^{-1}$	168	406	1631	788	1549

[a] Incoming solar ($K\downarrow$) and longwave ($L\downarrow$) flux densities W m^{-2} measured at quarry site, given for the 28.3-min time period (Δt) during the overflights. Standard deviation for $K\downarrow$ was 6 W m^{-2}, and for $L\downarrow$, 2 W m^{-2}.

Table 2. Sensitivity Analysis for the Variables Used To Calculate the Thermal Response Number

Variable[a]	*Quarry*	*Clrcut*	*Plant*	*Natreg*	*Maturef*
$\Delta\alpha = 0.05$	7.5	7.4	6.0	6.1	5.8
$\Delta\varepsilon = 0.01$	1.4	1.2	0.6	0.7	0.5
$\Delta R_n = 50\ \mathrm{W\ m^{-2}}$	11.2	9.7	6.5	6.9	6.0
$\Delta T = 0.2°\mathrm{C}$	0.3	0.3	0.2	0.2	0.1

[a] Results are given in percent change in TRN for a given change (error) in a single variable.

the canopy is warming or cooling would differences in R_n partitioning among LE, H, and G become evident. Therefore, the TRN, which is an expression of energy required to change T, could distinguish the site types.

A sensitivity analysis was performed on the TRN (Table 2) to identify what effect errors in the input variables (α, ε, R_n, ΔT) would have on the TRN. Generally the percent change in the TRN was small for a given change in all the variables. The TRN is most sensitive to changes in α and R_n. However, surface type influenced the sensitivity of the TRN most. Surfaces which had the least canopy cover were very sensitive to changes in all the variables. There was little difference among the forested surfaces. A reduction in ε of 0.02 would result in only a $\approx 1\%$ change in the TRN for the MATUREF site.

There are various implications of using the TIMS in studying landscape ecology and forest management. Effects of altering the land's surface on the microclimate and hydrologic cycle have been difficult to evaluate at a regional or watershed type scale. Gossmann (1986) calculated statistics of surface temperature for a combination of forested, agricultural, and urban land-use types using the uncalibrated thermal band on the Heat Capacity Mapping Mission (HCMM) satellite. He estimated that a 20% change in area from one land-use type to another would give a temperature change of up to 2.6–2.8°C. Another is the well-documented urban heat island effect which has been found to influence precipitation and regional energy balances (Oke, 1978). The variability in such areas is so great that conventional micrometeorologic techniques could not adequately characterize the thermal response of these surfaces.

CONCLUSIONS

Results of this study indicate that the TRN, derived from average surface temperatures and radiation balance estimates, is a site-specific surface property which can discriminate among various types of coniferous forest stands. The TRN provides an analytical framework for studying the effects of surface thermal response for large spatial resolution map scales that can be aggregated for input to smaller scales, as needed by global climate models. The sensitivity analysis showed that even with minimal ground based measurements, the TRN could separate the thermal response of several different forest types. With the advent of calibrated multipass satellite thermal sensors, and with the required atmospheric correction, it will be possible to study the thermal response of many other forest types. These landscape studies might include forest thermal cover type classification, cold air drainage patterns, examinations of the impact of drought, of excess moisture, or of insect damage on forests. In tropical areas, the effects of large scale deforestation on regional water and thermal balances could be examined. Future studies using the TRN should include various types of deciduous and tropical forests combined with more detailed information on stand characteristics such as basal area, leaf area index, and canopy biomass in order to identify their influence on the TRN.

This work was funded by NASA's Terrestrial Ecosystems program (RTOP # 677-21-29-03). The authors wish to thank the following Lockheed-LESC employees for their numerous and valuable contributions to this project; Bill Colliver, pilot; Duane O'Neal, TIMS operator; Julius Baham, data processing; and Sharon Hatch, data preparation.

REFERENCES

Anderson, J. E. (1985), Thermal infrared data: its characteristics and use, *Amer. Soc. Photogramm. Remote Sens. Technol.* Paper 1:143–155.

Aston, A. R. (1985), Heat storage in a young eucalypt forest, *Agric. Forest Meteorol.* 35:281–297.

Balick, L. K., and Wilson, S. K. (1980), Appearance of irregular tree canopies in nighttime high-resolution thermal infrared imagery, *Remote Sens. Environ.* 10:299–305.

Carlson, T. N. (1986), Regional-scale estimates of surface moisture availability in thermal inertia using remote thermal measurements, *Remote Sens. Rev.* 1:197–247.

Carson, D. J. (1982), Current parameterization of land-surface processes in atmospheric general circulation models, in *Land Surface Processes in Atmospheric General Circulation Models* (P. S. Eagleson, Ed.), pp. 67–108.

Childs, S. W., Holbo, H. R., and Miller, E. L. (1985), Shadecard and Shelterwood modification of the soil temperature environment, *Soil Sci. Soc. Am. J.* 49:1018–1023.

Dickinson, R. E. (1983), Land surface processes and climate-surface albedos and energy balance, *Adv. Geophys.* 25:305–353.

Fritschen, L. J., Balick, L. K., and Smith, J. A. (1982), Interpretation of infrared nighttime imagery of a forested canopy, *J. Appl. Meteorol.* 21:730–734.

Garnier, B. J., and Ohmura, A. (1968), A method of calculating the direct shortwave radiation income of slopes, *J. Appl. Meteorol.* 7:796–800.

Gates, D. M. (1962), *Energy Exchange in the Biosphere*, Harper and Row, New York, 151 pp.

Gossmann, H. (1986), The influence of geography on local environment as inferred from night thermal infrared imagery, *Remote Sens. Rev.* 1:249–275.

Hatfield, J. L., Reginato, R. J., and Idso, S. B. (1984), Evaluation of canopy temperature-evapotranspiration models over various surfaces, *Agric. Forest Meteorol.* 32:41–53.

Hawk, G. M., Franklin, J. F., McKee, W. A., and Brown, R. B. (1978), H. J. Andrews Experimental Forest reference stand system: establishment and use history, IBP Conif. Forest Biome Bull. No. 12, 79 pp.

Heilman, J. L., Kanemasu, E. T., Rosenberg, N. J., and Blad, B. L. (1976), Thermal scanner measurement of canopy temperatures to estimate evapotranspiration, *Remote Sens. Environ.* 5:137–145.

Hirsch, S. N., Kruckeberg, R. F., and Madden, F. H. (1971), The bi-spectral forest fire detection system, in Proc 9th Symp. Remote Sensing of Environment, Michigan Inst. & Science and Technology, University of Michigan, Ann Arbor, pp. 2253–2272.

Holbo, H. R., and Childs, S. W. (1987), Summertime radiation balances of clearcut and shelterwood slopes, *Forest Sci.* 33(2):504–516.

Holbo, H. R., Childs, S. W., and McNabb, D. H. (1985), Solar radiation at seedling sites below partial canopies, *Forest Ecol. Manage.* 10:115–124.

Ho, D. (1987), A soil thermal model for remote sensing, *IEEE Trans. Geosci. Remote Sens.* GE-25(2):221–229.

Idso, S. B., Jackson, R. D., and Reginato, R. J. (1975), The utility of surface temperature measurements for the remote sensing of surface soil water status, *J. Geophys. Res.* 80(21): 3044–3049.

Idso, S. B., Jackson, R. D., and Reginato, R. J. (1977), Remote sensing of crop yields, *Science* 189:1012–1013.

Jackson, R. D., Reginato, R. J., and Idso, S. B. (1977), Wheat canopy temperatures: A practical tool for evaluating water requirements, *Water Resour. Res.* 13:651–656.

Jarvis, P. G., James, G. B., and Landsberg, J. J. (1976), Coniferous forest, in *Vegetation and the Atmosphere* (J. L. Monteith, Ed.) Academic, New York, Vol. 2, pp. 171–240.

Kahle, A. B. (1987), Surface emittance temperature and thermal inertia derived from Thermal Infrared Multispectral Scanner (TIMS) data for Death Valley California, *Geophysics* 52(77):858–874.

Kneizys, F. X., Settle, E. P., Gallery, W. O., Chetwynd, J. H., Abreu, L. W., Selby, J. E. A., Fenn, R. W., and McClatchey, R. A. (1983), Atmospheric transmittance/radiance: computer code Lowtran-6, Air Force Geophysics Laboratory Rep. AFGL-TR83-0187, Optical Physics Division, Hanscom Air Force Base, MA 01731, 200 pp.

McCaughey, J. L. (1985), Energy balance storage terms in a mature mixed forest at Petawawa, Ontario—a case study, *Boundary-Layer Meteorol.* 31:89–101.

McCaughey, J. L. (1987), the albedo of a mature mixed forest and clear-cut site at Petawawa, Ontario, *Agric. Forest. Meteorol.* 40:251–263.

Monteith, J. L. (1973), *Principles of Environmental Physics*, Edward Arnold, London, 241 pp.

Moore, C. J. (1976), Eddy flux measurements above a pine forest, *Quart. J. Roy. Meteorol. Soc.* 102:913–918.

Moore, C. J. and Fisch, G. (1986), Estimating heat storage in Amazonian tropical forest. *Agric. Forest Meteorol.* 38:147–169.

Oke, T. R. (1978), *Boundary Layer Climates*, Wiley, New York, 372 pp.

Palluconi, F. D. and Meeks, G. R. (1985), Thermal infrared multispectral scanner (TIMS): An investigator's guide to TIMS data, JPL Pub. 85-32, 14 pp.

Pohn, H. A., Offield, T. W., and Watson, K. (1974), Thermal Inertia mapping from satellite-discrimination of geologic units in Oman, J. Res. U.S. Geol. Surv. 2(2):147–158.

Price, J. C. (1977), Thermal inertia mapping: a new view of the earth, *J. Geophys. Res.* 82(18):2582–2590.

Price, J. C. (1980), The potential of remotely sensed thermal infrared data to infer surface soil moisture and evaporation, *Water Resour. Res.* 16:787–795.

Price, J. C. (1982), Estimation of regional scale evapotranspiration through analysis of satellite thermal-infared data, *IEEE Trans. Geosci. Remote Sens.* GE-20(3):286–292.

Reginato, R. J., Jackson, R. D., and Pinter, P. J. (1985), Evapotranspiration calculated from remote multispectral and ground station meteorological data, *Remote Sens. Environ.* 18:75–89.

Sader, S. A. (1986), Analysis of effective radiant temperatures in a Pacific Northwest forest using thermal infrared multispectral scanner data, *Remote Sens. Environ.* 19:105–115.

Schieldge, J. P., Kahle, A. B., Alley, R. E., and Gillespie, A. R. (1980), Use of thermal-inertia properties for material identification, in *Image Processing for Missile Guidance*, *Soc. of Photo-Opt. Instrum. Eng.* 238:350–357.

Seguin, B., and Itier, B. (1983), Using midday surface temperature to estimate daily evaporation from satellite thermal IR data, *Int. J. Remote Sens.* (4)2:371–383.

Sellers, W. D. (1965), *Physical Climatology*, Univ. of Chicago Press, Chicago, 272 pp.

Shukla, J., and Mintz, Y. (1982), Influence of land-surface evapotranspiration on the earth's climate, *Science* 215:1498–1501.

Soer, G. J. R. (1980), Estimation of regional evapotranspiration and soil moisture conditions using remotely sensed crop surface temperatures, *Remote Sens. Environ.* 9:27–45.

Stewart, J. B., and Thom, A. S. (1973), Energy budgets in pine forest, *Quart. J. Roy. Meteorol. Soc.* 99:154–170.

Stone, L. R., and Horton, M. L. (1974), Estimating evapotranspiration using canopy temperatures: field evaluation, *Agron. J.* 66:450–454.

Sweat, M. E., and Carroll, J. (1983), On the use of spectral radiance models to obtain irradiances on surfaces of arbitrary orientation, *Solar Energy* 30(4):373–377.

Taylor, S. E. (1979), Measures emissivity of soils in the Southeast United States, *Remote Sens. Environ.* 8:359–264.

Thom, A. S. (1975), Momentum, mass and heat exchange of plant communities, in *Vegetation and the Atmosphere* (J. L. Monteith, Ed.), Academic, New York, Vol. 1, pp. 57–109.

Vanderwaal, J. A., and Holbo, H. R. (1984), Needle-air temperature differences of Douglas-fir seedlings and relation to microclimate, *Forest Sci.* 30(3):635–644.

Wilson, S. B., and Anderson, J. M. (1986), The applicability of LOWTRAN5 computer code to aerial thermographic data correction, *Int. J. Remote Sens.* 7(3):379–388.